π-cation-radical species, i.e. $(a_{1u}{}^2a_{2u}{}^1)$ for the $^2A_{2u}$ state and $(a_{2u}{}^2a_{1u}{}^1)$ for the $^2A_{1u}$ state. The effect of the order of the top-filled MO's, $(a_{1u}{}^2a_{2u}{}^1)$ vs $(a_{2u}{}^2a_{1u}{}^1)$, on the excited states accessed under resonance conditions has not yet been examined as a possible source of the discrepancy in sensitivities between resonance Raman and optical spectral data. Additionally, while the resonance Raman spectra pick up the major differences in molecular structure between TPP and OEP ring systems, it is perhaps possible that the resonance Raman spectrum does not pick up changes as well within a single geometry.

In summary, MCD spectra discriminate between ground states in porphyrin π-cation-radical species possibly because the reversal of the a_{1u}/a_{2u} order significantly changes the orbitals within the excited states. The spectra in Figures 4, 5, and 6B,C correspond to the porphyrin complexes in which a_{2u} is the highest occupied MO for the π-cation-radical species. This type of spectrum is common for ZnTPP(-1) and Co(II)- and Co(III)-containing porphyrin π-cation radicals with ClO_4^- and $SbCl_6^-$ counterions. These a_{2u} π-cation-radical species exhibit a similar scrambling in the visible region but maintain an almost normal Soret region band that arises from the mostly unaffected $a_{1u} \rightarrow e_g$ transition.

The absorption and MCD spectra for MgOEP(-1) and $[Co^{III}OEP(-1)]^{\bullet 2+}(Br^-)_2$ shown in Figures 6A and 10A, respectively, are clearly not the same as the spectra recorded for ZnTPP(-1), our model for the $^2A_{2u}$ ground state. Some similarities exist between these spectral data and the resolved spectra observed for MgPc(-1) complexes[51] in which the ground state is clearly $^2A_{1u}$. The $^2A_{1u}$ species are characterized by the well-resolved lowest energy band first associated with the spectrum of catalase compound I.[8]

Acknowledgment. We wish to acknowledge financial support from the NSERC of Canada through Operating, Strategic and Equipment grants and the Academic Development Fund at the UWO for an equipment grant. We thank Dr. William R. Browett for his contribution to the early stages of this work. This is publication No. 433 of the Photochemical Unit at the UWO. We are associated with the Centre for Chemical Physics and the Photochemical Unit at the UWO.

---

(51) Ough, E.; Gasyna, Z.; Stillman, M. L. Submitted for publication in *Inorg. Chem.*

Contribution from the Departments of Biophysics and Chemistry, University of Rochester, Rochester, New York 14642,
and The Squibb Institute for Medical Research, New Brunswick, New Jersey 08903-0191

Proton Magnetic Relaxation Dispersion in Aqueous Glycerol Solutions of $Gd(DTPA)^{2-}$ and $Gd(DOTA)^-$

Griselda Hernandez,[‡] Michael F. Tweedle,[§] and Robert G. Bryant*,[†,‡]

Received November 17, 1989

Nuclear magnetic relaxation rates are reported as a function of the magnetic field strength over the range of proton Larmor frequencies from 0.01 to 200 MHz for aqueous glycerol solutions of $Gd(DTPA)^{2-}$ and $Gd(DOTA)^-$ ions. The data are qualitatively described by the Solomon-Bloembergen-Morgan equations but are not described in detail by these equations. The effects of viscosity on the water proton relaxation efficiency are studied in particular to gain a better understanding of the dynamical factors controlling relaxation. The response of the nuclear relaxation to changes in the solution viscosity is a function of magnetic field strength because of compensating changes in the contributions of the rotational correlation times of the metal complexes and the electron spin-relaxation times to the effective correlation time for the electron-nuclear interaction.

Magnetic resonance imaging provides a safe and noninvasive imaging modality that is particularly useful for soft tissue discrimination. The basis for the contrast in the magnetic image is largely dominated by the differences in nuclear magnetic relaxation times among tissues.[1] Control of relaxation by spectroscopic or chemical means thus provides an additional diagnostic dimension that may be very useful in the identification of certain pathologies. Chelate complexes of gadolinium ion have been widely examined in this context because the high magnetic moment, labile coordinated water, and long electron spin-lattice relaxation times of this ion make these complexes generally efficient relaxation agents for the water proton spins in aqueous systems.[2,3] Currently, the most widely used complex is $Gd(DTPA)^{2-}$ (DTPA is diethylenetriaminepentaacetic acid);[4] however, other complexes such as $Gd(DOTA)^-$ (DOTA is 1,4,7,10-tetraazacyclododecane-1,4,7,10-tetraacetic acid) are more efficient in relaxing water proton spins. Both of these complexes are reported to provide one inner-sphere water molecule that exchanges rapidly with the solvent and couples the relaxation efficiency of the metal center to the whole solvent population.[5] Because these complexes are important representatives of a class of complexes, we report here nuclear magnetic relaxation dispersion measurements on highly purified materials as a function of the solution viscosity. This series of measurements displays the major features of the relaxation mechanisms operative in these complex ions and points to the important interplay between the electron spin-relaxation contribution to the correlation times for the electron-nuclear coupling and the rotational correlation time for the metal complex.

Experimental Section

Nuclear magnetic relaxation measurements were made on a field cycling spectrometer described elsewhere[6] that switches magnetic field strengths in real time from values limited by the earth's magnetic field to a proton Larmor frequency of 42 MHz. The relaxation rates were extracted from 16, 24, or 30 data points that were fitted to an exponential using a nonlinear least-squares procedure. The statistical errors were typically about 1%, though reproducibility was more nearly 5%. Samples were contained in 10-mm Pyrex sample tubes sealed with rubber stoppers and a screw cap. Temperature in the measurement coil was maintained by a flow of liquid perchloroethylene that was thermostated in an external Neslab RTE-8 temperature controller, which serviced the sample region by using outboard Little Giant pumps. Magnetic spin-lattice relaxation rates were also measured at a proton Larmor frequency of 200 MHz on a spectrometer described elsewhere.[7]

[†] Department of Biophysics, University of Rochester.
[‡] Department of Chemistry, University of Rochester.
[§] The Squibb Institute for Medical Research.

(1) Mansfield, P.; Morris, P. G. *NMR Imaging in Biomedicine*; Academic Press: New York, 1982.
(2) Koenig, S. H.; Brown, R. D., III. *Magn. Reson. Med.* **1984**, *1*, 478.
(3) Lauffer, R. B. *Chem. Rev.* **1987**, *87*, 901.
(4) Wainmann, H. J.; Brasch, R. C. *AJR, Am. J. Roentgenol.* **1984**, *142*, 619.
(5) Bryden, C. C.; Reilley, C. N. *Anal. Chem.* **1982**, *54*, 610.
(6) Hernandez, G.; Brittain, H. G.; Tweedle, M. F.; Bryant, R. G. *Inorg. Chem.* **1990**, *29*, 985.
(7) Jackson, C. L.; Bryant, R. G. *Biochemistry* **1989**, *28*, 5024.

0020-1669/90/1329-5109$02.50/0

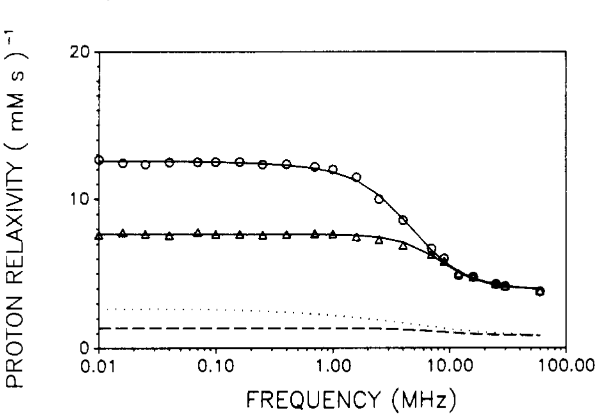

Figure 1. Water proton millimolar nuclear magnetic spin-lattice relaxivity as a function of the magnetic field strength plotted as the proton Larmor frequency for Gd(DOTA)$^-$ (O) and Gd(DTPA)$^{2-}$ (Δ) at pH 7 and 298 K. The solid lines were computed by using eqs 1–5 after taking the outer-sphere contributions into account, which are shown as dotted and dashed lines respectively.

Na[Gd(DOTA)H_2O]·4H_2O was prepared by dissolving 1 mol of H_5DOTA (Parish Chemical Co., Oren, UT; 539 g corrected for 25 weight percent sulfate and moisture) and 0.5 mol (181 g) of Gd_2O_3 were mechanically stirred in about 1.5 L of distilled water in a 2 L flask at 368 K for 6.5 h. After the mixture was cooled to room temperature, 1 mol (40 g) of NaOH was slowly added with stirring. Further NaOH was then added until most of the solid dissolved, and the pH was 7. After the mixture was filtered through a medium-coarse frit, water was rotatory evaporated and replaced with acetone to precipitate the solid product. The solubility of the sodium salt is about 0.7 M in water. After the first precipitate was collected by filtration, 470 g, more acetone was added and a second crop collected, about 90 g (83%). Both crops were recrystallized from hot water/acetone. Anal. Calcd: H_2O, 13.9; C, 28.49; H, 5.10; N, 8.31. Found: H_2O, 13; C, 28.23; H, 4.96; N, 8.37. Free gadolinium ion was estimated at less than 0.02 mol %, and free DOTA, at less than 0.06% by UV at 280 nm detected HPLC titration of Cu(DOTA): 150 mm Hamilton PRP-x100 column, in 1.25 mM Tris acetate, 2.5 mM Na_2EDTA, pH 7.3, 2% acetonitrile, 15% methanol at a flow rate of 2 mL/min.[8] Retention times were 2.5 min for Cu(DOTA) and 4.0 min for Cu(EDTA).

Na_2[Gd(DTPA)H_2O]·7H_2O was prepared by treating 410 g of H_5DTPA (Aldrich) and 0.5 mol (181 g) of Gd_2O_3 as above, heating for only 2 h. The solubility of the product in water is about 1 M. A total of 494 g was collected (84% yield). Anal. Calcd: H_2O, 18.8; C, 23.09; H, 4.59; N, 5.77. Found: H_2O, 23; C, 22.97; H, 4.01; N, 5.73. Free gadolinium ion was less than 0.02 mol %, and free DTPA was less than 0.25%. The retention time for Cu(DTPA) is only slightly different from that of Cu(EDTA).

Solutions were made by weight using 20 mM aqueous phosphate buffer as the solvent. Viscosity measurements were made with an Ubbelohde viscometer utilizing the same solutions measured in the NMR experiments.

Results and Discussion

The paramagnetic contributions to the nuclear magnetic relaxation dispersion are shown in Figure 1. These data are qualitatively similar to those presented by Geraldes and coworkers[9] and in quantitative agreement with the data presented by Sherry and co-workers.[10]

Most magnetic relaxation dispersion data is qualitatively described by equations developed by Bloembergen, Solomon, and Morgan[11-13]

$$(1/T_{1m}) = \{(2/15)\gamma_I^2\gamma_s^2S(S+1)/r^6\}\{3\tau_{c1}/(1+\omega_I^2\tau_{c1}^2) + 7\tau_{c2}/(1+\omega_s^2\tau_{c2}^2)\} + \{(2/3)S(S+1)\,(A/\hbar)^2\}\{\tau_{2e}/(1+\omega_s^2\tau_{2e}^2)\} \quad (1)$$

where γ_I and γ_s are the nuclear and electron magnetogyric ratios, ω_I and ω_s are the Larmor frequencies for the nuclear and electron spins, $\hbar$ is Planck's constant divided by 2π, r is the distance from the metal center of a hydrated ion to a proton of hydration, S is the spin of the paramagnetic ion, A is the electron–proton hyperfine coupling constant and the correlation times are given by eqs 2 and 3, where τ_{rot} is the rotational correlation time of the

$$\tau_{ck}^{-1} = \tau_{rot}^{-1} + \tau_{ex}^{-1} + \tau_{sk}^{-1} \qquad k = 1, 2 \quad (2)$$

$$\tau_{2e}^{-1} = \tau_{ex}^{-1} + \tau_{s2}^{-1} \quad (3)$$

intermoment vector, τ_{ex} is the mean lifetime of the nucleus in the paramagnetic environment, and τ_{s1} and τ_{s2} are the electron spin longitudinal and transverse relaxation times respectively. The electron relaxation times are generally dependent on the magnetic field strength. This dependence may be complicated because a number of interactions may contribute to shifts in the electron resonance frequency and the electron relaxation rates.[14-16] We assume here the simplest model[9,12,17,18] for the electron relaxation rates given by eqs 4 and 5, where B is a constant proportional to

$$1/\tau_{s1} = B\tau_v[1/(1+\omega_s^2\tau_v^2) + 4/(1+4\omega_s^2\tau_v^2)] \quad (4)$$

$$1/\tau_{s2} = B\tau_v[1.5 + 2.5/(1+\omega_s^2\tau_v^2) + 1/(1+4\omega_s^2\tau_v^2)] \quad (5)$$

the strength of the interaction driving relaxation, which is assumed to be the zero-field splitting in most cases, and τ_v is a correlation time that modulates this interaction. These equations neglect any contribution from the electron–metal–nucleus hyperfine coupling that may contribute to a spread of electron resonance frequencies.[19,20] The electron spin resonance line width of these complexes measured in 1 mM aqueous solutions at 298 K was found to be 713 and 92 G for the Gd(DTPA)$^{2-}$ ion and Gd(DOTA)$^-$ ion, respectively. These widths are in excess of the anticipated hyperfine splittings for gadolinium complexes. Thus, neglect of this contribution to the relaxation equation is justified.

The relatively efficient nuclear spin relaxation induced by both complexes implies that the electron spin-relaxation times are not very short compared with the rotational correlation time of the metal complexes, which is consistent with the magnetic behavior of the f^7 ions in general. The shape of the relaxation dispersion plots is Lorentzian for both complexes as shown in Figure 1; i.e., the observable field dependence of the relaxation rate may be described well by just the ω_s terms of eq 1. The absence of a low-frequency inflection, which is observed in aqueous solutions of ions such as hexaaquomanganese(II),[21,22] indicates that the hyperfine coupling constant between the electrons of the metal center and the protons of the labile water molecules must be small. An alternative explanation is that the electron–proton hyperfine coupling is large but the electron relaxation time is very short. This condition would move the dispersion from the hyperfine contribution to high frequency; however, were this the case, the electron relaxation time would have to be on the order of the rotational correlation time of the metal complex or about 50 ps. This possibility is inconsistent with the line width of the EPR spectrum and the viscosity dependence of the water proton relaxation rate. Therefore, it seems very likely that the electron-water proton hyperfine coupling is small, which is consistent with the unpaired electrons residing in the well-shielded f orbitals.[23,24]

---

(8) Hagan, J. J.; Cicero, S. C.; Tweedle, M. F. *Anal. Chem.* **1988**, *60*, 514.
(9) Geraldes, C. F. G. C.; Sherry, A. D.; Brown, R. D., III; Koenig, S. H. *Magn. Reson. Med.* **1986**, *3*, 242.
(10) Sherry, A. D.; Brown, R. D., III; Geraldes, C. F. G. C.; Koenig, S. H.; Kuan, K.-T.; Spiller, M. *Inorg. Chem.* **1989**, *28*, 620.
(11) Solomon, I. *Phys. Rev.* **1955**, *99*, 559.
(12) Bloembergen, N. *J. Chem. Phys.* **1957**, *27*, 572.
(13) Bloembergen, N.; Morgan, L. O. *J. Chem. Phys.* **1961**, *34*, 842.
(14) Gregson, A. K.; Dodrell, D. M.; Pegg, D. T. *Aust. J. Chem.* **1978**, *31*, 469.
(15) Poupko, R.; Baram, A.; Luz, A. *Mol. Phys.* **1974**, *27*, 1345.
(16) Kowalewski, J.; Nordenskiold, L.; Benetis, N.; Westlund, P. O. *Prog. Nucl. Magn. Reson. Spectrosc.* **1985**, *17*, 141.
(17) McLachlan, A. D. *Proc. R. Soc. London, A* **1964**, *280*, 271.
(18) Rubinstein, M.; Baram, A.; Luz, Z. *Mol. Phys.* **1971**, *20*, 67.
(19) Bertini, I.; Briganti, F.; Koenig, S. H.; Luchinat, C. *Biochemistry* **1985**, *24*, 6287.
(20) Banci, L.; Bertini, I.; Briganti, F.; Luchinat, C. *J. Magn. Reson.* **1986**, *66*, 58.
(21) Hauser, R.; Noack, F. *Z. Phys.* **1964**, *182*, 93.
(22) Koenig, S. H.; Brown, R. D., III. *Magn. Reson. Med.* **1984**, *1*, 478.

Table I. Relaxation Parameters for Gadolinium Complexes

ligand	r, Å	τ_{rot}, ps	τ_{s2},[a] ns
DOTA	2.9	48	11
DTPA	2.9	48	0.35

[a] For magnetic field strength corresponding to a proton Larmor frequency of 0.01 MHz.

The outer-sphere contribution to the water proton spin relaxation is considered in detail elsewhere[25-27] and may be computed from an estimate of the distance of closest approach of a water molecule to the paramagnetic center, b, and the relative translational diffusion constant for water and the metal complex, which has been found to vary little from the diffusion constant of bulk water.[25] Computations using this approach for the outer-sphere contribution where the distance of closest approach is 5.88 Å and the diffusion constant is 2.1×10^{-5} cm^2 s^{-1} are shown as the dashed and dotted lines for Gd(DTPA)$^{2-}$ and Gd(DOTA)$^-$, respectively, in Figure 1. The complete estimate of the outer-sphere contribution requires an estimate of the electron spin-relaxation times, which in the present cases are larger than the rotational correlation times for the complexes at low magnetic field strengths. The strategy utilized involved simultaneous computation of the outer-sphere contribution and the first-coordination-sphere contributions, though they are separated for clarity in Figure 1. We note, however, that for the present complexes the contribution of the electron relaxation times to the effective correlation times for the outer-sphere relaxation is small because the translational correlation times are much shorter. The solid lines in Figure 1 were computed by using eqs 1–5 after accounting for the outer-sphere contribution, and the parameters obtained are summarized in Table I.

For the DOTA complex, the low-frequency relaxation rate compared to the high-frequency rate is approximately consistent with the prediction of Solomon's theory that 70% of the relaxation efficiency should be lost because of the ω_s dispersion. This approximate correspondence to Solomon's theory is expected if the electron spin-relaxation time is long compared to the rotational correlation time in the DOTA complex, thus making little contribution to the effective correlation times for the interaction. This result is supported by reasonable agreement between the value of the correlation time for the electron spin relaxation derived for the DOTA complex and the EPR line width. For the DTPA complex, however, the amplitude of the relaxation dispersion does not change by 70% as suggested by Solomon's equations. In this case, the electron spin-relaxation time is shorter than for the DOTA complex as shown by the increase in the EPR line width as well as the entry in Table I. The effect of the shorter electron relaxation time is to cause a shorter effective correlation time for the electron–nuclear interaction that results in a lower nuclear spin-relaxation rate. However, the electron relaxation time is field dependent, increasing with increasing field strength. At high fields, the electron relaxation time increases, the rotational contributions to the effective correlation time are dominant, and the relaxation rates observed for the water protons are similar for the two complexes.

Several additional features of the data are of note: (1) The intermoment distances that scale the magnitude of the low-frequency relaxation rates agree well with the structural chemistry of aquo ion complexes in general; i.e., the distance of approximately 2.9 Å is consistent with that in similar complexes.[28,29] (2) The rotational correlation time of approximately 50 ps is close to the correlation times found for other complex ions of this size in water.[30] (3) The chemical exchange time, τ_{ex}, does not make a significant contribution to the effective correlation time for the electron–nuclear interactions driving the nuclear spin relaxation, which is consistent with the lability of gadolinium complexes in general.[31,32] (4) The electron relaxation time, τ_{s2}, derived from the fit to the data is not very well determined because the contribution to the effective correlation time is not dominant. However, the electron relaxation time is clearly shorter in the Gd(DTPA)$^{2-}$ case than in the Gd(DOTA)$^-$ case and for Gd(DTPA)$^{2-}$ ion appears to be approximately 10% of the contribution to the effective correlation time in eq 2 on the basis of the parameters that fit the shapes of the relaxation dispersion curves.

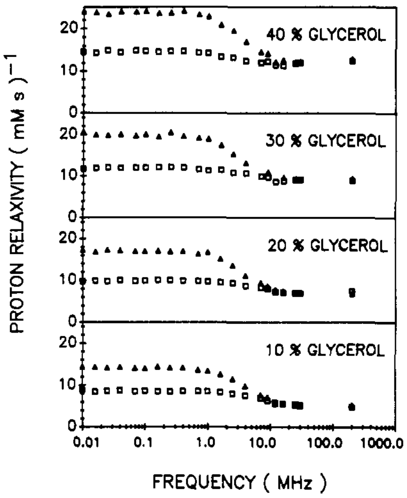

Figure 2. Water proton millimolar nuclear magnetic spin–lattice relaxivity as a function of the magnetic field strength plotted as the proton Larmor frequency for Gd(DOTA)$^-$ (△) and Gd(DTPA)$^{2-}$ (□) at pH 7 and 298 K for solutions containing 10, 20, 30, and 40 wt % glycerol.

The viscosity dependence of the nuclear magnetic relaxation dispersion is of considerable practical interest because the administration of relaxation control agents in vivo may involve different dynamical environments. Further, the viscosity dependence provides fundamental information about the competing contributions to the relaxation equation.

The water proton–nuclear spin relaxivities are shown as a function of solution viscosity for the Gd(DOTA)$^-$ ion and Gd(DTPA)$^{2-}$ in Figure 2 where viscosity has been adjusted by using glycerol. For both complexes, the nuclear spin-relaxation rates increases with the glycerol concentration. At low magnetic field strengths, the complexes have rather different relaxation efficiencies. Furthermore, this difference increases with increasing viscosity. However at high magnetic field strengths, the relaxation efficiency becomes very similar.

Quantitative prediction of these effects is difficult because of the major approximations made in the relaxation equations, and because of the difficulty of modeling the microdynamic viscosity accurately from measurements of the bulk viscosity.[33-35] Inspection of eqs 4 and 5 indicates that the electron relaxation times become long at high magnetic field strengths because the $\omega_s\tau_c$ products are large. A consequence is that contributions of the electron spin relaxation to eq 2 may be neglected and the effective correlation time for the electron–nuclear interaction becomes the rotational correlation time. The relaxivities measured at 200 MHz of the Gd(DOTA)$^-$ and the Gd(DTPA)$^{2-}$ ions are nearly identical at all viscosities. The sizes of these ions are very similar and their rotational correlation times will be nearly identical as a consequence. Thus, the high-field relaxivity implies not only that the

---

(23) Koenig, S. H.; Epstein, M. *J. Chem. Phys.* **1975**, *63*, 2279.
(24) Koenig, S. H.; Baglin, C.; Brown, R. D., III. *Magn. Reson. Med.* **1984**, *1*, 496.
(25) Lester, C. C.; Bryant, R. G. *J. Phys. Chem.* **1990**, *94*, 3654.
(26) Polnaszek, C. F.; Bryant, R. G. *J. Chem. Phys.* **1984**, *81*, 4038.
(27) Freed, J. H. *J. Chem. Phys.* **1978**, *68*, 4034.
(28) Narten, A. H.; Hahn, R. L. *Science* **1982**, *217*, 1249.
(29) Spirlet, M. R.; Rebizant, J.; Desreux, J. F.; Loncin, M. F. *Inorg. Chem.* **1984**, *23*, 359.
(30) Bertini, I.; Lucinat, C. *NMR of Paramagnetic Molecules in Biological Systems*; Benjamin/Cummings: Menlo Park, CA, 1986.
(31) Southwood-Jones, R. V.; Earl, W. L.; Newman, K. E.; Merbach, A. E. *J. Phys. Chem.* **1980**, *73*, 5909.
(32) Cossy, C.; Helm, L.; Merbach, A. E. *Inorg. Chem.* **1989**, *28*, 2699.
(33) Lee, M.; Bain, A. J.; McCarthy, P. J.; Han, C. H.; Haseltine, J. N.; Smith, A. B., III; Hochstrasser, R. M. *J. Chem. Phys.* **1986**, *85*, 4341.
(34) Bloembergen, N.; Purcell, E. M.; Pound, R. V. *Phys. Rev.* **1948**, *73*, 679.
(35) Debye, P. *Polar Molecules*; Dover Publications: New York, 1945.

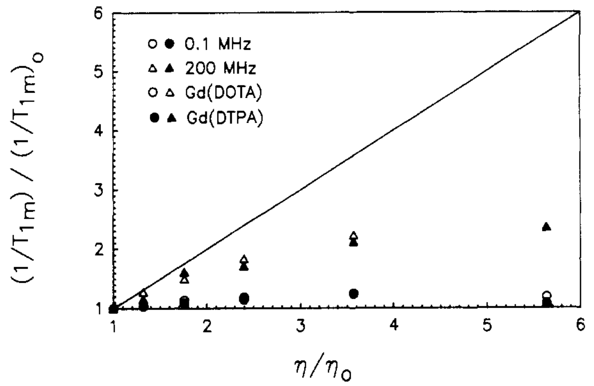

Figure 3. Water proton nuclear magnetic spin–lattice relaxivity normalized to the relaxivity with no glycerol as a function of the normalized viscosity at 0.1 and 200 MHz, pH 7, and 298 K.

rotational correlation times are the same for the two complexes but also, because the number of exchanging water molecules is reported to be the same, the water proton–gadolinium distance must be the same as well. Since the geometrical factors do not change with the solution viscosity, the observed dependence of the relaxation rate on the viscosity may be attributed to the dependence of the rotational correlation time on the viscosity. The data in Figure 3 show the water proton nuclear magnetic spin–lattice relaxivity normalized to the relaxivity of the glycerol free solution as a function of the viscosity normalized the same way. The dependence is not linear with unit slope as predicted by the Stokes–Einstein–Debye model; however, similar observations have been reported based on measurements of the decay of fluorescence anisotropy.[36–38]

The linewidth of the electron spin resonance spectrum for the Gd(DOTA)$^-$ ion, which is practically independent of solution viscosity, implies that the electron spin-relaxation time, T_2, is on the order of 7×10^{-10} s or longer measured at the X-band, which corresponds to approximately 8 MHz in Figure 1. The relaxation time will be this long or longer at 200 MHz, which supports the conclusion that the correlation time appropriate to the high-field relaxation is the rotational correlation time only. Further, this conclusion should be valid throughout the viscosity range studied. Thus, the data for the Gd(DOTA)$^-$ complex provides a measure of the microdynamic viscosity of the solution as a function of the glycerol concentration. As mentioned above, the rotational correlation time is not a linear function of the bulk viscosity; however, the rotational correlation time is independent of magnetic field strength. The rotational correlation times derived from the high-field relaxation data may be used to attempt to understand the differences between the low-field relaxation rates.

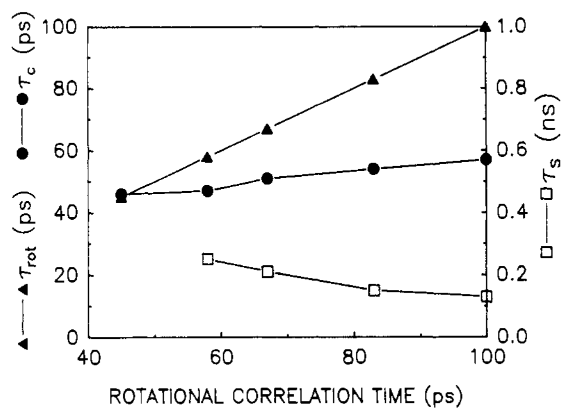

Figure 4. Correlation times for the Gd(DOTA)$^-$ ion. The rotational correlation times are obtained from the water proton spin–lattice relaxation time at 200 MHz. The effective correlation time and the electron spin-relaxation time were obtained from the water proton relaxation data at 0.1 MHz as described in the text.

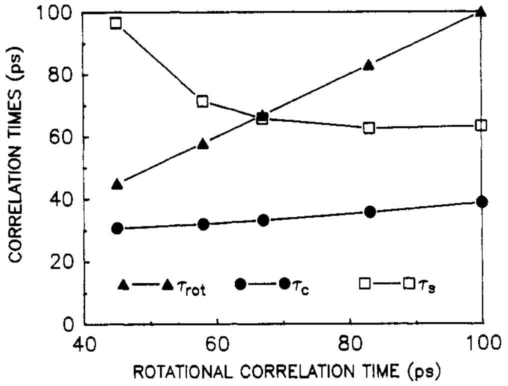

Figure 5. Correlation times for the Gd(DTPA)$^{2-}$ ion. The rotational correlation times are obtained from the water-proton spin–lattice relaxation time at 200 MHz. The effective correlation time and the electron spin-relaxation time were obtained from the water proton relaxation data at 0.1 MHz as described in the text.

The data in Figure 3 demonstrate that at low magnetic field strengths, the effective dependence of the paramagnetic contribution to the water proton relaxation rate on viscosity is very weak. The only difference between the high-field and the low-field magnetic relaxation involves the contributions associated with the electron spin-relaxation rates to the effective correlation times. There are a number of problems associated with modeling the relaxation rates at low field, because the details of the electron relaxation equation as a function of field are difficult to model. Some simplifications appear possible, however. At low magnetic field strength, the differences between the longitudinal and transverse electron relaxation rates should be minimized. Furthermore, the denominators in eq 1 become unity, and the equation becomes the strength of the dipolar coupling times the effective correlation time. We assume that the outer-sphere contribution to relaxation scales with the contribution calculated for the glycerol-free solutions; that is, the outer-sphere contribution remains a constant fraction of the total relaxation rate. Since the outer-sphere contribution depends on the relative translational motion of the water and the metal complex, the outer-sphere contribution should increase linearly with increasing microdynamic viscosity. The rotational correlation times deduced from the 200-MHz data and the effective correlation times at low field deduced by using these assumptions are shown in Figures 4 and 5 for the Gd(DOTA)$^-$ and Gd(DTPA)$^{2-}$ complexes, respectively. It is obvious that in both cases the effective correlation time for the electron–nuclear coupling at low field increases only slightly while the rotational correlation time increases by more than a factor of 2 over the range of viscosities studied. The difference between the rotational and effective correlation times at low field are generally associated with contributions from the electron relaxation times. Application of eq 2 yields the electronic contribution, which is shown in Figures 4 and 5. Qualitatively, these graphs emphasize the obvious, that is, that there are compensating changes in the electron relaxation times that attenuate the increase in relaxivity expected on the basis of increases in the rotational correlation time. For the Gd(DOTA)$^-$ complex, where the Solomon equation is nearly satisfied, the values of the electronic contribution to an effective correlation time provides a measure of the viscosity dependence of the electronic relaxation rates. However, eq 2 and the analysis used assume that the electron-relaxation rate contributes independently to the fluctuations in the local fields experienced by the nuclei relaxed. We have no assurance that this assumption is valid for either complex studied here. The NMR data and this elementary analysis do lead to predictions on the magnitudes of the electron spin-relaxation times that are not inconsistent with the EPR measurements. Indeed, even for the Gd(DTPA)$^{2-}$ complex, where the rotational correlation time is on the order of the electron relaxation contributions even at 8 MHz, the contribution of the electron relaxation rate to the NMR

---

(36) Rice, S. A.; Kenney-Wallace, G. A. *Chem. Phys.* **1980**, *49*, 161.
(37) Chuang, T. J.; Eisenthal, K. B. *Chem. Phys. Lett.* **1971**, *11*, 368.
(38) Canonica, S.; Schmid, A. A.; Wild, V. P. *Chem. Phys. Lett.* **1985**, *122*, 529.

relaxation does match the EPR line width measured. The extrapolation of this situation to lower magnetic field strengths, however, is complex because eq 1 may be incorrect.[39,40] We report this simple approach because it does provide an estimate of the electronic contributions to the low magnetic field relaxation rates and may provide an indication of the dependence of the electron relaxation properties on the dynamical characteristics of the solution or when the complex is attached to a macromolecule. In this spirit, we note that, for both complexes, the electronic contributions to the correlation time increase with increasing viscosity, though the dependence is weaker even than that of the rotational correlation time.

In summary, the nuclear magnetic relaxation dispersion profiles for both the $Gd(DOTA)^-$ and $Gd(DTPA)^{2-}$ ions are described by a Lorentzian shape, which implies that an exponential correlation function is adequate to describe the fluctuations in the electron–nuclear coupling. Further, the high-field relaxation rate is dominated by the rotational motions in both complexes which are within experimental error the same. The high-field data have provided a direct measure of the rotational correlation times of the complexes as a function of solution viscosity that provides an opportunity to examine the low-field contributions by knowing the magnitude of the rotational correlation times. This analysis has provided an estimate of the electron spin-relaxation rates. The electron relaxation rates increase with increasing microdynamic viscosity, but not in the same proportion as the rotational correlation time. Thus, major changes in the dynamical environment of a paramagnetic metal center may not lead to significant changes in the efficiency of induced nuclear spin relaxation because of compensating changes in the contributions to the effective correlation time for the electron–nuclear coupling.

Acknowledgment. This work was supported by the National Institutes of Health (Grant GM39309), The University of Rochester, and the Squibb Institute for Medical Research. We also acknowledge the synthetic and analytical work of A. Krumwiede and S. C. Taylor.

---

(39) Bertini, I.; Luchinat, C.; Mancini, M.; Spina, G. *J. Magn. Reson.* **1984**, *59*, 213.

(40) Bertini, I.; Luchinat, C.; Kowalewski, J. *J. Magn. Reson.* **1985**, *62*, 235.

Contribution from the Departamento de Química,
Faculdade de Ciências do Porto, 4000 Porto, Portugal

EPR and Electrochemical Study of Nickel(III) Complexes of Bis(3,5-dichlorosalicylaldehyde) *o*-Phenylenediimine. Evidence for Adduct Formation with Pyridines

Baltazar de Castro* and Cristina Freire

Received January 11, 1990

Electrochemical oxidation of [bis(3,5-dichlorosalicylaldehyde) *o*-phenylenediiminato]nickel(II), $[Ni(3,5\text{-}Cl_2saloph)]$ (**1**), was performed in DMF and $(CH_3)_2SO$. In these strong donating solvents (S) the Ni(II) complex is oxidized to a Ni(III) complex (low-spin d^7 electron configuration), which can be formulated as $[Ni(3,5\text{-}Cl_2saloph)\cdot S_2]^+$. Upon addition by pyridines to freshly electrolyzed solutions of compound 1, novel electron paramagnetic resonance (EPR) spectra indicate the formation of new paramagnetic species, the species formed depending on the basic strength of the pyridines added. Thus, for the weaker bases, the EPR spectra indicate the presence of new Ni(III) species ($g_{av} \approx 2.12$) with the bases (B) coordinated axially ($[Ni(3,5\text{-}Cl_2saloph)\cdot B_2]^+$), whereas for the more strongly basic pyridines, the unpaired electron is transferred into the equatorial ligand, forming Ni(II) ligand radical complexes ($g = 2.00$). The analysis of the EPR parameters of Ni(III)–pyridine adducts suggests that the adducts have a d_{z^2} ($^2A_1$) ground state and also accounts for the observed g_z values, in excess relative to that of the free electron, as being due to the influence of low lying quartet states. The application of the same model to the analysis of the spin Hamiltonian parameters of the EPR spectra of $[Ni(3,5\text{-}Cl_2saloph)\cdot S_2]^+$, shows that it has a d_{z^2} ground state and yields values of $E(d_{xz},d_{yz} \rightarrow d_{z^2})$ in good agreement with those obtained from the electronic spectra.

Introduction

The recognition that the less-common oxidation states of nickel, Ni(III) and Ni(I), play a crucial role in the activity of several hydrogenases,[1a,b] of methyl coenzyme M reductase,[1c,d] and of carbon monoxide oxydoreductase (CO dehydrogenase)[1e,f] has spurred intense activity in the synthesis and characterization of Ni(III) and Ni(I) complexes.[1h] This activity has centered on the requirements for the stabilization of d^7 and d^9 electronic configurations for nickel and, particularly for complexes of the former, on factors that determine the relative stability of the Ni(III) complexes compared to Ni(II) radical complexes.[2]

There is accumulated evidence[3–5] that in the oxidation of Ni(II) square-planar complexes, where ligand-localized oxidation is also accessible, the final oxidation site (metal or ligand) depends on the ability of the solvent (or of other donors present in solution) to stabilize the high metal oxidation state through axial ligation. For macrocyclic or other π delocalized square-planar complexes, where the π energy levels of the ligand and those of the central Ni(II) ion are very similar, axial coordination can shift the d_{z^2} orbital above the filled ligand orbitals, thus making metal oxidation the preferred process. However in the absence of strong axial interactions, oxidation will probably result in the loss of an electron from the ligand-based π system.

Nickel(II) bis(salicylaldiimine) complexes provide good examples of systems where the oxidation potential of the ligands and of the complexes do not differ appreciably and where a large solvent dependence for the ultimate oxidation site is observed. In acetonitrile, and in other weak donor solvents (donocity number

---

(1) (a) Lancaster, J. R. *FEBS Lett.* **1980**, *115*, 285. (b) Albracht, S. P. J.; Graft, E.-G.; Thauer, R. K. *FEBS Lett.* **1982**, *140*, 311. (c) Gunsalus, R. P.; Wolfe, R. S. *FEMS Microbiol. Lett.* **1978**, *3*, 191. (d) Diekert, G.; Klee, B.; Thauer, R. K. *Arch. Microbiol.* **1980**, *124*, 103. (e) Pfaltz, A.; Juan, B.; Fässler, A.; Eschenmoser, A.; Jaenchen, R.; Gilles, H. H.; Diekert, G.; Thauer, R. R. K. *Helv. Chim. Acta* **1982**, *65*, 828. (f) Diekert, G.; Thauer, R. R. K. *J. Bacteriol.* **1978**, *136*, 597. (g) Diekert, G.; Graft, E.-G.; Thauer, R. R. K. *Arch. Microbiol.* **1979**, *122*, 117. (h) The bioinorganic aspects of nickel have been reviewed recently in *The Bioinorganic Chemistry of Nickel*; Lancaster, J. R., Jr., Ed.; VCH Publishers: New York, 1988.

(2) Lappin, A. G.; McAuley, A. *Adv. Inorg. Chem.* **1988**, *32*, 241.

(3) Kapturkiewicz, A.; Behr, B. *Inorg. Chim. Acta* **1983**, *69*, 247.

(4) Chavan, M. Y.; Meade, T. J.; Busch, D. H.; Kuwana, T. *Inorg. Chem.* **1986**, *25*, 314.

(5) Goldsby, K. A.; Blaho, J. K.; Hoferkamp, L. A. *Polyhedron* **1989**, *8*, 113.

0020-1669/90/1329-5113$02.50/0